Midwall Shortening After Coarctation Repair: The Effect of Through-plane Motion on Single-plane Indices of Left Ventricular Function

Thomas L. Gentles, FRACP, Brett R. Cowan, MB, ChB, Christopher J. Occleshaw, FRCR, Steven D. Colan, FACC, and Alistair A. Young, PhD, *Auckland, New Zealand; and Boston, Massachusetts*

Left ventricular midwall function is increased after repair of coarctation of the aorta (CoA). The cause is unclear. This study aimed to examine the variance between fiber shortening derived from 3-dimensional models of myocardial deformation, and 1- and 2-dimensional indices of left ventricular systolic function. In all, 15 young adults after CoA and 15 matched control subjects were recruited. Endocardial and midwall fractional shortening were calculated using M-mode echocardiography. Ejection fraction, midwall fractional shortening, and myocardial deformation were calculated or measured from magnetic resonance (MR) imaging. Echocardiographic and cine-MR imaging midwall fractional shortening were increased after CoA ($P = .02$ and $<.001$). In contrast, 3-dimensional MR tagging demonstrated normal midwall circumferential shortening and decreased longitudinal shortening in the CoA group ($P < .01$). Cine MR midwall shortening, recalculated to allow for through-plane motion, was similar to tagged midwall shortening, with no difference between the CoA and control groups. After CoA, measures of left ventricular function systematically overestimate midwall fiber shortening unless the methodology accounts for through-plane motion. (J Am Soc Echocardiogr 2005;18:1131-1136.)

Endocardial ejection phase indices of myocardial performance (fractional shortening [FS] and ejection fraction) are augmented in patients with concentric hypertrophy and concentric remodeling as a geometric consequence of increased relative wall thickness.[1,2] Midwall fiber shortening is a better indicator of average fiber shortening under these circumstances and geometric midwall fiber tracking formulae have been advocated for this purpose.[2] These formulae derive an estimate of midwall fiber shortening from M-mode echocardiographic measurements of left ventricular (LV) cavity and wall dimension. A number of investigators have demonstrated impaired midwall fiber shortening in patients with concentric hypertrophy despite normal endocardial shortening indices.[2-4] Furthermore, impaired midwall shortening is an independent predictor of cardiovascular events in patients with hypertensive heart disease,[5] where it is closely associated with abnormal diastolic function.[6]

We recently studied M-mode–derived endocardial and midwall shortening in a group of children and young adults who had increased LV mass (LVM) after repair of coarctation of the aorta (CoA).[7] Endocardial FS (FS_{EN}) was increased, as was midwall shortening, albeit to a lesser extent. Although increased endocardial shortening can be explained on the basis of concentric hypertrophy, the cause of increased midwall shortening is not clear. This is particularly so as these findings are at variance with those from animal and human studies, where chronic hypertrophy is associated with depressed midwall shortening.[2]

We hypothesized that the increase in midwall shortening seen in this patient group is artifactual: related to the use of fixed reference, single-plane imaging, and exacerbated by regional variation in mass and shortening. Because systematic disparities between 1- and 2-dimensional (2D) indices of LV function and myocardial fiber shortening may have important clinical consequences given the prognos-

From the Green Lane Paediatric and Congenital Cardiac Service, Starship Children's Hospital, Auckland, New Zealand (T.L.G., C.J.O.); Department of Cardiology, Children's Hospital, Boston, Massachusetts (S.D.C.); Department of Pediatrics, Harvard Medical School, Boston, Massachusetts (S.D.C.); and Departments of Anatomy (A.A.Y.), Medicine (B.R.C.), and Paediatrics (T.L.G.), University of Auckland, Auckland, New Zealand.

Supported by grant funding from the National Heart Foundation of New Zealand and the Auckland Medical Research Foundation, and an Equipment Grant from the Welcome Trust (United Kingdom).

Reprint requests: Thomas L. Gentles, FRACP, Green Lane Paediatric and Congenital Cardiac Service, Starship Children's Hospital, Private Bag 92-024, Auckland 1001, New Zealand (E-mail: *tomg@adhb.govt.nz*)

0894-7317/$30.00

doi:10.1016/j.echo.2005.05.004

tic importance of myocardial dysfunction in hypertensive heart disease,[5] midwall myocardial shortening was calculated from magnetic resonance (MR) imaging (MRI) tissue tagging measurements in a group of young adults late after repair of CoA. We then compared these measurements with indices of LV function derived from 1-dimensional and 2D echocardiography and MRI.

METHODS

Patient Population

The study population consisted of 15 young adults who had undergone repair of CoA 17 to 23 years previously. Those with hemodynamically significant cardiac lesions were excluded prospectively; two patients with trivial aortic stenosis and regurgitation, and one with a tiny muscular ventricular septal defect, were included. In addition, 15 age-, sex-, and body size–matched healthy participants were recruited as control subjects. The study protocol was approved by the regional ethics committee and informed consent was obtained from each participant.

Echocardiograms

Echocardiographic examinations were undertaken with a cardiac imager (Sonos 1500, Hewlett-Packard, Andover, MA) and included a standard 2D, pulsed, continuous wave, and color Doppler examination to assess the aortic arch and to exclude any intracardiac anomalies. An M-mode examination of the LV short axis at the level of the tip of the mitral valve leaflets and simultaneous phonocardiogram were recorded on hard copy over 3 to 5 cardiac cycles. This was subsequently digitized using customized software.[8] End diastole (ED) was defined as the largest dimension and end systole (ES) as the onset of the second heart sound on the phonocardiogram. The relative wall thickness was calculated as ED posterior wall thickness (EDPosth)/EDD where EDD is the ED LV short-axis cavity dimension, and LVM was calculated using the formula of Devereux and Reichek [9]:

$$\mathrm{LVM} = 0.83\,[(\mathrm{EDD} + \mathrm{EDPosth} + \mathrm{EDSepth}) - (\mathrm{EDD})^3] + 0.6 \quad (1)$$

where EDSepth is the thickness of the septum at ED.

FS_{EN} was calculated as: (EDD − ES dimension [ESD])/EDD × 100. LV ED midwall dimension was calculated as: EDD + Edh, where EDh is the average of the septal wall thickness at ED and EDPosth. The LV midwall ESD was calculated using the formula described by Shimizu et al,[10] geometrically tracking the midwall fiber identified at ED to its position at ES:

$$\mathrm{ESD_{MW}} = [(\mathrm{ESD})^2 + \mathrm{ESh}(2\mathrm{EDD} + \mathrm{EDh})(\mathrm{ESD} + \mathrm{ESh})/(\mathrm{EDD} + \mathrm{EDh})]^{0.5} \quad (2)$$

where ESD_{MW} is the midwall ESD, and where ESh and EDh are the wall thickness at ES and ED, respectively (equal to the average of the septum and posterior wall thickness). Midwall FS (FS_{MW}) was calculated in a similar fashion to FS_{EN}.

MRI

All imaging was performed using a 1.5-T magnet (Vision, Siemens Medical Systems, Erlangen, Germany) with a phased-array surface coil. Cineimages and tagged images were obtained using sequences reported previously.[11,12] The tag spacing in the orthogonal grid pattern was 8 mm and the tag lines were oriented at 45 degrees relative to the imaging axes. A set of 6 long-axis tagged image slices was also acquired at equal 30-degree increments around the LV central axis (with 3 of these slices coinciding with the long-axis untagged cineslices). Good-quality image stripes were obtained throughout systole in all slices.

LV Volume

ED volume, ES volume, and myocardial wall volume were determined interactively from the untagged images using guide-point modeling.[13] Volumes were calculated from the model using numeric integration. LVM was calculated from the average of the myocardial volumes at ED and ES, multiplied by the specific gravity of myocardium (1.05 g/mL).

Geometric Midwall Shortening

For calculation of geometric midwall shortening fraction, the endocardial and epicardial borders of the short-axis slice, two thirds to three quarters of the distance from the apex to the base, were digitized at ED and ES. This slice (slice 6 of 8 or 9 slices) was chosen to correspond approximately to the level of echocardiographic M-mode imaging. Dimensions were derived from cross-sectional area and the FS_{MW} was calculated using the same formulae as were used for the echocardiographic M-mode midwall function analysis. However, there is substantial longitudinal (L) displacement of the myocardium from the base to the apex at this level of the LV, such that the myocardium imaged at ED moves out of the imaging plane by the time of ES. This displacement is approximately one slice spacing (8-11 mm). To allow for through-plane motion in the geometric measurement of midwall shortening, the adjacent basal slice (slice 7) was digitized at ED, and FS_{MW} was recalculated using dimensions derived from slice 7 at ED and slice 6 at ES.

Tag Tracking and Reconstruction of 3-dimensional Deformation

Tag stripes were semiautomatically tracked using a previously described and validated technique.[14,15] The geometry and deformation of the LV was reconstructed with the aid of a finite element model, as described previously.[14,15] The model interpolated the displacement constraints between tag and image planes, resulting in a consistent 3-dimensional (3D) displacement field. The percentage shortening or lengthening of myocardium was calculated

Table 1 Study population

	Coarctation	Control	*P* value
Age, y	23.5 (3.3)	23.2 (2.6)	.74
M:F sex	11:4	11:4	1.00
BSA, m^2	1.9 (0.2)	1.8 (0.3)	.79
R arm systolic BP, mm Hg	132 (14)	117 (12)	<.01
Systolic arm-leg gradient	11.5 (12.8)	−13.1 (8.9)	<.01

BSA, body surface area; *BP*, blood pressure; *F*, female; *M*, male; *R*, right.
Mean (SD).

as the change in length as a percentage of the ED length in the circumferential (C) and L directions:

$$\%S_A = \frac{dl_{ED} - dl_{ES}}{dl_{ED}} \cdot 100\% \quad (3)$$

where A is one of the C or L directions, $\%S_A$ is the percentage shortening or lengthening at time in this direction, and dl_{ED} and dl_{ES} are the lengths of an infinitesimal material line segment (oriented in this direction at ED) at ED and ES, respectively. ES was taken to be the time of least model cavity volume in the tagged model reconstruction. Because C shortening is known to increase toward the apex,[15] shortening of the midwall circumference was derived from the 3D model at a level similar to the untagged cine short-axis image used to calculate geometric midwall shortening (ie, at the level of echocardiographic M-mode imaging). L shortening was averaged through the ventricle and twist was calculated as the angle of rotation about the central axis from ED to ES relative to the base.

Statistical Analysis

Results are summarized as mean (SD) unless otherwise stated. Intergroup relationships were examined using a 2-tailed Student *t* test, and relationships between variables were examined by linear regression analysis. A *P* value of .05 or less was considered statistically significant.

RESULTS

Patient Characteristics

Body surface area, age, and sex were closely matched, but the CoA group had a significantly higher systolic blood pressure and arm-leg systolic blood pressure gradient compared with control subjects (Table 1). The residual systolic upper to lower body blood pressure gradient ranged from 0 to 30 mm Hg (median 9 mm Hg) in the CoA group.

LV Geometry

There was no difference in LV chamber size between the CoA and control groups either by echocardiographic M-mode (ED dimension) or MRI (ED volume) (Table 2). The echocardiographic M-mode EDPosth and mass were increased in the CoA group and there was a trend toward an increased MRI mass. Both echocardiographic M-mode ED relative wall thickness and the MRI mass:volume ratio were increased, indicating concentric remodeling.

Table 2 Left ventricular geometry

		Coarctation	Control	*P* value
Echo				
	EDD, cm/m^2	2.9 (0.3)	2.8 (0.3)	.91
	EDPosth, cm/m^2	0.50 (0.07)	0.42 (0.05)	<.01
	Mass, g/m^2	97 (15)	83 (18)	.03
	EDPosth/D	0.175 (0.022)	0.150 (0.016)	<.01
MRI				
	EDV, mL/m^2	78 (13)	77 (8.9)	.68
	Mass, g/m^2	95.6 (14.2)	87.2 (10.1)	.07
	Mass/EDV	1.23 (0.12)	1.14 (0.10)	.04

Echo, Echocardiography; *EDD*, end-diastolic dimension; *EDPosth*, end-diastolic posterior wall thickness; *EDPosth/D*, end-diastolic posterior wall: chamber dimension ratio; *EDV*, end-diastolic volume; *MRI*, magnetic resonance imaging.
Mean (SD).

Table 3 Left ventricular function indices

		Coarctation	Control	*P* value
Echo				
	FS_{EN}, %	37.3 (4.9)	33.1 (4.6)	.02
	FS_{MW}, %	21.1 (3.3)	18.1 (2.6)	.01
MRI				
	EF, %	65.3 (4.5)	60.8 (1.9)	<.01
	FS_{MW1}, %	21.4 (2.7)	19.6 (2.3)	.05
	FS_{MWT2}, %	19.0 (3.3)	18.7 (2.4)	.74

Echo, Echocardiography; *EF*, ejection fraction; FS_{EN}, endocardial fractional shortening; FS_{MW}, midwall fractional shortening; *FSMW*, midwall fractional shortening; FS_{MW1}, midwall fractional shortening calculated from the same slice at end systole and end diastole; FS_{MWT2}, midwall fractional shortening calculated from the adjacent basal slice in end diastole to allow for through-plane motion; *MRI*, magnetic resonance imaging.

LV Function Indices

Indices of LV chamber function (echocardiographic M-mode FS_{EN} and MR ejection fraction) were elevated in the CoA group (Table 3). FS_{MW} was elevated in the CoA group when calculated from echocardiographic M-mode images and from similarly positioned MRI 2D short-axis images. However, there was no difference between the CoA and control groups when MRI FS_{MW} was recalculated to correct for through-plane motion related to L shortening by using the adjacent basal slice in ED.

MRI Tag-derived Fiber Shortening

Global averages of 3D tag-derived C and L shortening through time are reported elsewhere.[12] When averaged over the midwall third of the ventricle, C shortening was similar in both groups (20.8 [1.4] vs 20.7 [1.1]%, P = not significant) (Figure 1), as was

shortening at the midwall circumference at a level corresponding to that of the M-mode echocardiography (19.4 [2.4] vs 19.5 [1.7]%, P = not significant). In contrast, L shortening was significantly decreased in the CoA group (14.9 [1.3] vs 16.8 [1.4]%, $P < .01$), whereas average twist of the apex and midventricle relative to the base about the L axis was increased (9.9 [1.4] vs 8.7 [1.7] degrees, $P = .04$) (Figure 1).

Influence of LV Geometry on Shortening Indices

The M-mode echocardiographic FS_{EN} was related to the MRI tag-derived C midwall shortening and to the relative wall thickness ($r = 0.61$, $P < .01$), indicating this index of chamber function was influenced not only by C shortening, but also by concentric remodeling. In contrast, there was no relationship between the relative wall thickness and MRI tag-derived C midwall shortening ($P = .50$), indicating that average midwall fiber shortening is independent of ventricular geometry.

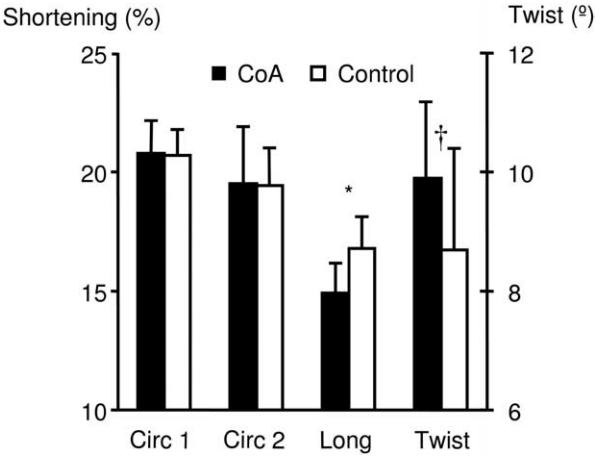

Figure 1 Circumferential shortening of midwall third of left ventricle (*Circ 1*) and of midwall circumference (*Circ 2*), longitudinal shortening (*Long*), and twist from magnetic resonance imaging tissue tag 3-dimensional model. *$P < .01$ and †$<.05$ CoA compared with control subjects.

DISCUSSION

The failure of endocardial indices of LV function to accurately reflect midwall or average fiber shortening in the presence of concentric remodelling and concentric hypertrophy is well recognized, particularly in the context of hypertensive heart disease[5,16] and calcific aortic stenosis,[17] where significant myocardial dysfunction may be present despite normal indices of endocardial shortening. Increased LV endocardial and midwall function have been reported after CoA repair, where there is also a high incidence of concentric hypertrophy and remodelling.[18-20] Although increased endocardial incursion during systole can be explained as a geometric consequence of concentric remodelling, increased midwall shortening cannot. The primary aim of this study was to investigate possible causes of this apparent increase in LV midwall function. Endocardial and midwall indices of LV function were elevated in those who had undergone CoA repair regardless of imaging modality. In contrast, the 3D tissue tag model demonstrated normal shortening of the midwall circumference and of the entire midwall third of the LV. This 3D model tracks material points of myocardium through systole and into early diastole. As such it accounts for through-plane motion, and provides a measure of myocardial shortening that is independent of geometric assumptions. It has been validated in phantoms and yields accurate estimates of strain at any vector.[14,15]

The misrepresentation of midwall fiber shortening by endocardial or chamber function indices was related to the relative wall thickness and, thus, exacerbated by concentric remodeling and concentric hypertrophy. Incompressible models that predict an increase in both ejection fraction and endocardial shortening with constant midwall fiber shortening and increasing hypertrophy explain this phenomenon.[1,2] Because chamber function is not representative of average fiber function, the geometric formula described by Shimizu et al[2,10] is frequently used to estimate midwall shortening fraction from M-mode echocardiographic recordings.

We calculated midwall shortening from M-mode recordings and from MRI 2D short-axis images at a similar level in the LV. Both estimates of midwall shortening were elevated in the coarctation group, a finding reported by ourselves[24] and others[21] in larger patient groups. Explanations for this finding include an altered inotropic state, perhaps related to neurohormonal abnormalities,[22,23] decreased afterload, or a limitation of the model used to calculate midwall shortening. Although wall stress is known to be reduced after CoA repair, we recently discussed the failure of conventional wall stress measurements to account for abnormal relative wall thickness.[24] Using fiber stress, a measure of afterload that accounts for intramural forces in addition to chamber forces,[25] we found afterload to be normal after CoA repair.[24] Thus, increased midwall shortening is difficult to explain at a mechanical level. In the current study the finding of enhanced midwall function was at variance with the MR tissue tag results where the CoA and control groups had virtually identical midwall C shortening. This suggests that the increase in geometric midwall shortening indices in the CoA group is artifactual.

The formula used to calculate midwall shortening from the 1-dimensional echocardiographic and 2D

MR images (equation 2) models the LV as a cylinder and assumes conservation of myocardial mass through the cardiac cycle. The ED midwall fiber is tracked to ES on the assumption that any increase in cross-sectional area of the short axis of the LV is accounted for by shortening about the L axis. As short-axis area is generalized to the entire length of the cylindric model, regional mass and shortening are assumed to be homogenous and the myocardium imaged in systole is assumed to be representative of that imaged in diastole. LV regional shortening is known to be heterogeneous,[12,15,26] and this may also be the case for regional mass distribution. Therefore, measurements taken from a single imaging plane are not necessarily representative of average LV geometry. This problem will be exacerbated by an inability to account for through-plane motion, and may be a particularly important source of error in the LV with concentric hypertrophy where L shortening and twist are abnormal.[12,15,27]

Because of this theoretic concern we corrected for through-plane motion by recalculating the midwall shortening analysis using the next basal slice at ED. Given that L displacement is approximately 10 mm,[28] the slice imaged at ES will correspond approximately to the adjacent basal slice at ED. Interestingly, the results of this analysis show midwall shortening to be no different in the coarctation group compared with control subjects. Moreover, absolute values of shortening were similar to those obtained from MR tagging at the same level. It is important to note that L shortening and twist vary according to the mass:volume ratio.[12,29,30] Hence, when using a single imaging plane, the magnitude and vector of cardiac translation will be dependent on the degree of concentric hypertrophy. Discrepancy between single-plane and 3D measures of midwall function will also be related to the shape of the LV. If the cross-sectional area increases toward the base, a common pattern of hypertrophy in children and young adults, the midwall and global fiber shortening will be underestimated. Given the multiple factors involved, the magnitude of error introduced by single-plane imaging is unpredictable.

These findings indicate that the abnormal elevation of midwall shortening seen after CoA repair is a result of the failure of single-plane imaging to account for through-plane motion. Commonly used indices of midwall C function may systematically overestimate midwall shortening in the LV with increased relative wall thickness, if the imaging modality fails to account for myocardial translation in other planes. The magnitude of this overestimation (~10%) is not large, and its clinical significance unknown. Nevertheless, failure to detect impaired midwall shortening may have implications after CoA repair when decisions regarding reintervention for residual arch obstruction remain ill-defined,[31] and concerns persist regarding the long-term consequences of hypertension and LV hypertrophy.[32,33]

These findings may have implications for the assessment of LV function in other patient groups with concentric hypertrophy and concentric remodelling. Assessment of midwall function using imaging modalities that account for through-plane motion should be considered in those with concentric hypertrophy and low-normal midwall shortening estimated by the conventional M-mode formula.

REFERENCES

1. Dumesnil JG, Shoucri RM, Laurenceau JL, Turcot J. A mathematical model of the dynamic geometry of the intact left ventricle and its application to clinical data. Circulation 1979; 59:1024-34.
2. Shimizu G, Hirota Y, Kita Y, Kawamura K, Saito T, Gaasch WH. Left ventricular midwall mechanics in systemic arterial hypertension: myocardial function is depressed in pressure-overload hypertrophy. Circulation 1991;83:1676-84.
3. de Simone G, Devereux RB, Celentano A, Roman MJ. Left ventricular chamber and wall mechanics in the presence of concentric geometry. J Hypertens 1999;17:1001-6.
4. Sadler DB, Aurigemma GP, Williams DW, Reda DJ, Materson BJ, Gottdiener JS. Systolic function in hypertensive men with concentric remodelling. Hypertension 1997;30:777-81.
5. de Simone G, Devereux RB, Koren MJ, Mensah GA, Casale PN, Laragh JH. Midwall left ventricular mechanics: an independent predictor of cardiovascular risk in arterial hypertension. Circulation 1996;93:259-65.
6. Schussheim AE, Diamond JA, Jhang JS, Phillips RA. Midwall fractional shortening is an independent predictor of left ventricular diastolic dysfunction in asymptomatic patients with systemic hypertension. Am J Cardiol 1998;82:1056-9.
7. Gentles TL, Sanders SP, Colan SD. Misrepresentation of left ventricular contractile function by endocardial indices: clinical implications after coarctation repair. Am Heart J 2000;140: 585-95.
8. Colan SD, Parness IA, Spevak PJ, Sanders SP. Developmental modulation of myocardial mechanics: age- and growth-related alterations in afterload and contractility. J Am Coll Cardiol 1992;19:619-29.
9. Devereux RB, Reichek N. Echocardiographic determination of left ventricular mass in man: anatomic validation of the method. Circulation 1977;55:613-8.
10. Shimizu G, Zile MR, Blaustein AS, Gaasch WH. Left ventricular chamber filling and midwall fiber lengthening in patients with left ventricular hypertrophy: overestimation of fiber velocities by conventional midwall measurements. Circulation 1985;71:266-72.
11. Axel L, Dougherty L. Heart wall motion: improved method of spatial modulation of magnetization for MR imaging. Radiology 1989;172:349-50.
12. Young AA, Cowan BR, Occleshaw CJ, Oxenham H, Gentles TL. Temporal evolution of left ventricular strain late after repair of coarctation of the aorta using 3D MR tissue tagging. J Cardiovasc Magn Reson 2002;4:233-43.
13. Young AA, Cowan BR, Thrupp SF, Hedley WJ, Dell'Italia LJ. Left ventricular mass and volume: fast calculation with guide-point modeling on MR images. Radiology 2000;216: 597-602.

14. Young AA, Kraitchman DL, Dougherty L, Axel L. Tracking and finite element analysis of stripe deformation in magnetic resonance imaging. IEEE Trans Med Imaging 1995;14:413-21.
15. Young AA, Kramer CM, Ferrari VA, Axel L, Reichek N. Three-dimensional left ventricular deformation in hypertrophic cardiomyopathy. Circulation 1994;90:854-67.
16. Palmon LC, Reichek N, Yeon SB, Clark NR, Brownson D, Hoffman E, et al. Intramural myocardial shortening in hypertensive left ventricular hypertrophy with normal pump function. Circulation 1994;89:122-31.
17. Aurigemma GP, Silver KH, McLaughlin M, Mauser J, Gaasch WH. Impact of chamber geometry and gender on left ventricular systolic function in patients > 60 years of age with aortic stenosis. Am J Cardiol 1994;74:794-8.
18. Leandro J, Smallhorn JF, Benson L, Musewe N, Balfe JW, Dyck JD, et al. Ambulatory blood pressure monitoring and left ventricular mass and function after successful surgical repair of coarctation of the aorta. J Am Coll Cardiol 1992;20:197-204.
19. Carpenter MA, Dammann JF, Watson DD, Jedeikin R, Tompkins DG, Beller GA. Left ventricular hyperkinesia at rest and during exercise in normotensive patients 2 to 27 years after coarctation repair. J Am Coll Cardiol 1985;6:879-86.
20. Kimball TR, Reynolds JM, Mays WA, Khoury P, Claytor RP, Daniels SR. Persistent hyperdynamic cardiovascular state at rest and during exercise in children after successful repair of coarctation of the aorta. J Am Coll Cardiol 1994;24:194-200.
21. Pacileo G, Pisacane C, Russo MG, Crepaz R, Sarubbi B, Tagliamonte E, et al. Left ventricular remodeling and mechanics after successful repair of aortic coarctation. Am J Cardiol 2001;87:748-52.
22. Simsolo R, Grunfeld B, Gimenez M, Lopez M, Berri G, Becu L, et al. Long-term systemic hypertension in children after successful repair of coarctation of the aorta. Am Heart J 1988;115:1268-73.
23. Ross RD, Clapp SK, Gunther S, Paridon SM, Humes RA, Farooki ZQ, et al. Augmented norepinephrine and renin output in response to maximal exercise in hypertensive coarctectomy patients. Am Heart J 1992;123:1293-9.
24. Gentles TL, Colan SD. Wall stress misrepresents afterload in children and young adults with abnormal left ventricular geometry. J Appl Physiol 2002;92:1053-7.
25. Regen DM. Calculation of left ventricular wall stress. Circ Res 1990;67:245-52.
26. Bogaert J, Rademakers FE. Regional nonuniformity of normal adult human left ventricle. Am J Physiol Heart Circ Physiol 2001;280:H610-20.
27. Tongue AG, Dumesnil JG, Laforest I, Theriault C, Durand LG, Pibarot P. Left ventricular longitudinal shortening in patients with aortic stenosis: relationship with symptomatic status. J Heart Valve Dis 2003;12:142-9.
28. Rogers WJ Jr, Shapiro EP, Weiss JL, Buchalter MB, Rademakers FE, Weisfeldt ML, et al. Quantification of and correction for left ventricular systolic long-axis shortening by magnetic resonance tissue tagging and slice isolation. Circulation 1991;84:721-31.
29. Aelen FW, Arts T, Sanders DG, Thelissen GR, Muijtjens AM, Prinzen FW, et al. Relation between torsion and cross-sectional area change in the human left ventricle. J Biomech 1997;30:207-12.
30. Stuber M, Scheidegger MB, Fischer SE, Nagel E, Steinemann F, Hess OM, et al. Alterations in the local myocardial motion pattern in patients suffering from pressure overload due to aortic stenosis. Circulation 1999;100:361-8.
31. Attenhofer Jost CH, Schaff HV, Connolly HM, Danielson GK, Dearani JA, Puga FJ, et al. Spectrum of reoperations after repair of aortic coarctation: importance of an individualized approach because of coexistent cardiovascular disease. Mayo Clin Proc 2002;77:646-53.
32. Toro-Salazar OH, Steinberger J, Thomas W, Rocchini AP, Carpenter B, Moller JH. Long-term follow-up of patients after coarctation of the aorta repair. Am J Cardiol 2002;89:541-7.
33. Cohen M, Fuster V, Steele PM, Driscoll D, McGoon DC. Coarctation of the aorta: long-term follow-up and prediction of outcome after surgical correction. Circulation 1989;80:840-5.